Article

Experimental investigation of pier scour depth and its scour hole pattern for different shapes

Kaleem Afzal Khan[1,2], Muhammad Waseem[3], Mehtab Alam[1,4], Mujahid Khan[2], Megersa Kebede Leta[5,*]

[1] Department of Civil Engineering, Ghulam Ishaq Khan Institute of Engineering Sciences and Technology, Topi 23640, Pakistan

[2] Department of Civil Engineering, University of Engineering and Technology, Peshawar 25000, Pakistan

[3] School of Interdisciplinary Engineering & Sciences (SINES), National University of Sciences & Technology (NUST), Sector H-12, Islamabad 44000, Pakistan

[4] Department of Geotechnical Engineering, College of Civil Engineering, Tongji University, Shanghai 200092, China

[5] Faculty of Agriculture and Environmental Sciences, University of Rostock, 18059 Rostock, Germany

* Corresponding author: Megersa Kebede Leta, megersa.kebede@uni-rostock.de

Abstract: Local scour, a complex phenomenon in river flows around piers with movable beds, can damage bridge piers during high floods. Predicting scour depth accurately is vital for safety and economic reasons, especially for large bridges. This study using hydraulic flume laboratory experiments compared diamond, square, and elliptical pier models of different sizes under steady clear-water conditions considering different flow rates and discharge levels to identify the most efficient shape with less local scour. Local scour, a complex phenomenon in three-dimensional flow around piers in rivers with movable beds, can lead to detrimental effects on bridge piers due to high flood velocities. Accurate prediction of scour depth is crucial for economic and safety reasons, especially for large bridges with complex piers. Hydraulic engineers are keen on forecasting the equilibrium scour depth. To achieve this, laboratory testing compared diamond, square, and elliptical pier models under steady clear-water conditions to identify the most efficient pier shape with less local scour. This research provides valuable insights for optimizing pier design to enhance bridge stability and resilience against scour-induced risks. A variety of configurations, including different sizes and shapes of piers were experimented with in the flume using diamond, square, and elliptical shapes. The test results showed that the local scour depth around elliptical piers was around 29.16% less, and around diamond piers, it was approximately 16.05% less compared to the scour depth observed around square piers with the same dimensions. The researchers also observed distinct patterns of scouring around different pier shapes. Specifically, the square-shaped piers displayed the highest level of scouring depth, that is, 48 mm, followed by the diamond-shaped pier which experienced a scouring depth of 48 mm while the elliptical-shaped piers experienced the least amount of scouring depth, that is, 34 mm. The test results also demonstrated that pier size significantly influences scouring, with an increase in pier size from 3×3 cm2 to 5×5 cm2 leading to a rise in scour depth by 26.04%. Moreover, this study findings also elucidated that an increase in flow results in an increase of in scouring depth i.e., elevating the discharge from 0.0026 cumecs to 0.0029 cumecs led to a 28.13% increase in scouring depth for the identical pier size. These findings provide valuable insights into the hydraulic behavior of various pier shapes and can aid in the optimization of bridge design and hydraulic engineering practices. The investigations further revealed that local scouring is sensitive not only to pier dimensions but also to other critical parameters, including flow rate, time of exposure, and the size of a pier.

Keywords: local scour; bridge piers; hydraulic structures; different shaped pier; experimental investigation; flow rate

1. Introduction

The scouring of bridge piers is a critical concern when evaluating bridge safety (Shahriar et al., 2021). Scour, refers to the erosion-driven lowering of a channel bed below its natural level, potentially exposing or undermining foundations that would otherwise remain buried Research has shown that most bridge failures can be attributed to the scouring of foundation material (Zhang et al., 2022). The process of local scouring around bridge piers is utterly complex, influenced by a variety of factors like flow characteristics, pier traits, and bed material properties (Deng & Cai, 2010). Ensuring the safe and cost-effective design of bridges requires accurate prediction of scour depth around piers, making it of paramount importance.

Innovatively, leveraging advanced predictive models and cutting-edge technologies becomes imperative to accurately forecast scour depths around bridge piers, revolutionizing the safety and cost-effectiveness of bridge designs. During significant flood events, other factors like floating debris and debris accumulation further impact scouring (Panici & de Almeida, 2018).

Excessive scour poses substantial risks, leading to high maintenance costs or even bridge collapse. Such collapses result in costly repairs, traffic disruptions, and potential loss of life for bridge users (Heller, 2011). This mechanism can potentially compromise the structural integrity of bridges and hydraulic structures (**Figure 1**), leading to failure when the foundation is weakened (Masjedi et al., 2010).

Figure 1. The base of a pillar of Topi bridge has been exposed making it dangerous for traffic (https://www.dawn.com/news/1344788).

Scour events are particularly prevalent during floods and can trigger bridge collapses (Farooq et al., 2017). Scour is commonly categorized into two types: aggradation and degradation. Aggradation involves the gradual buildup of a channel bed's longitudinal profile due to sediment deposition, originating from the channel or the watershed upstream of the bridge. On the other hand, degradation refers to the long-term lowering of the channel bed caused by erosion over a relatively extended channel length. This process occurs when there is a deficit in sediment supply from upstream, leading to the scouring or lowering of the streambed (Sotiropoulos et al., 2012). Enhancing comprehension of local scour phenomena holds paramount importance for engineers tasked with designing piers and pile foundations. In the realm of modern bridge engineering, scour stands as a prominent factor contributing to bridge failures, thus commanding the utmost attention from engineers. Renowned

design codes, such as AASHTO (American Association of State Highway and Transportation Officials) (Kuchma et al., 2008), OHBDC (Oregon Hydraulic Basis Design Criteria) (Bakht & Jaeger, 1992), and CHBDC (Canadian Highway Bridge Design Code) (Eddine & Arjomandi, 2020), and HEC18 (Hydraulic Engineering Circular No. 18) include provisions for hydraulic design, recommending approved methods based on empirical equations (Lyn, 2008). However, these widely used equations tend to over-predict the depth of scour. Factors contributing to scour are diverse (see **Figure 2**), including channel geomorphology, flow transport, bed sediment, and bridge geometry (Aly & Dougherty, 2021). Scale effects, caused by modeling imbalances, also play a role in scour overestimation (Heller, 2011).
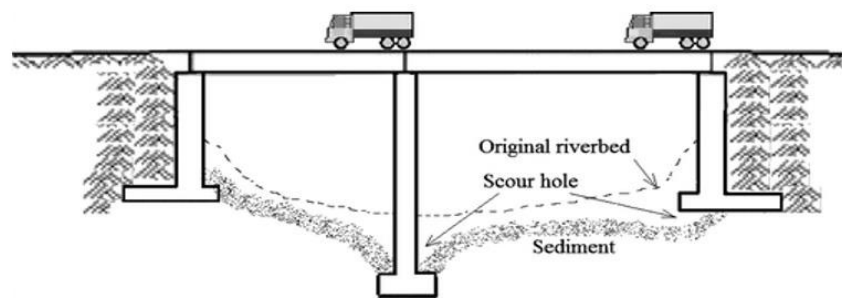
Figure 2. Impact of scouring (Deng & Cai, 2010).

Researchers have conducted numerous experimental and numerical studies to quantify the equilibrium depth of scour in different soil materials. Equations have been developed to predict scour depth, and extensive efforts have been made to understand the scouring mechanism.

The contemporary approach to predicting scour significantly relies on two influential hydraulic engineering circulars, HEC-18 (Lyn, 2008) and HEC-20 (Zevenbergen, 2010), authored respectively by Richardson and Davis (1995) and Lagasse et al. (1995). These publications, issued by the Federal Highway Administration (FHWA), serve as fundamental references shaping current practices in hydraulic engineering, particularly in scour prediction methodologies. Flow velocity, depth, and sediment size sequentially impact scour, yet graded materials with armor layers shift emphasis to sediment distribution. Notably, a comprehensive review elsewhere synthesizes prior research and scour-depth equations (Dargahi, 1982).

Dey (1997a, 1997b) presented insights into three-dimensional velocity distributions within an equilibrium scour hole around a circular pier. The studies provided a comprehensive review that amalgamated findings from both experimental and field studies, offering a synthesized understanding of the subject matter derived from empirical observations and theoretical frameworks. He employed a five-hole Pitot sphere to measure these velocities, contributing valuable data regarding flow patterns within such scour formations (Dey, 1997a, 1997b).

Ismail (2009) used a 1-D model for Aswan Bridge and found local scour depths of 13.66 m and 14.47 m for flow rates of 270 and 350 Mm^3/day, respectively. For El-Minia Bridge, the local scour depths were 1.81 m and 4.53 m for all piers with normal and 30° angle of attack at a flow rate of 181 Mm^3/day, respectively.

Lai et al. (2009) investigated the effects of varying flow on temporal scour using

flood or flow hydrographs. They derived an unsteady flow factor based on peak-flow intensity and time-to-peak of the hydrograph and developed relations to estimate (dse) for uniform bed material. Tests were conducted for steady flow and linearly rising followed by steady flow, showing that the rising portion of the hydrograph influences scours. Relations for predicting scour under unsteady flow conditions were established.

Beg (2010) studied the impact of bridge pier configuration on scour geometry. Considering piers as isolated during design neglects the flow interference effect, potentially leading to bridge failure. When centerline pier spacing was zero, the scour depth was 95% higher than an isolated pier of diameter. At pier spacing equal to D, the scour depth remained 1.21 times larger. However, with increasing spacing-to-D ratio, scour depth decreased until 8D spacing, resembling that of an isolated pier. Unsteady flow in natural flow systems presents a unique scouring situation, affecting both scour geometry and its temporal development.

Gampathi (2010) found that scour depth increases with the flow angle relative to the pier axis. Ismael et al. (2015) conducted experiments to study the effect of bridge pier position on reducing scour. They observed a 40% reduction in scour depth for normal piers and a 54.5% reduction for opposite piers compared to circular piers.

Tejada (2014) extensively studied flow channel blockage effects. Previous experiments used higher blockage ratios, possibly affecting empirical equation development for pier design. Scour depth increased in smaller flumes with higher blockage ratios, and even slight changes in the ratio of particle size (D) to the channel width (D/b) of 2.2% to 5% caused scour depth (dse) variations. Large blockage ratios notably influenced scour depth and geometry, particularly evident at small (D) to the median diameter of the sediment (D50) (D/D_{50}) values. Notably, when D/D50 < 100, HEC18 (Lyn, 2008) emerged as a viable design code, showcasing minimal impact on dse/D ratio.

Dahe and Kharode (2015) used the Hydrologic Engineering Center's River Analysis System (HEC-RAS) model to estimate scour depth for bridge piers and found that sharp nose-shaped piers had better values, while square-shaped piers had the highest scour depth (Brunner, 2016).

Chen et al. (2018) used two types of smart rocks, direction unknown (DU) and direction known (DK), to monitor bridge scour. By analyzing magnetic field interference, algorithms were created to locate these rocks amidst varying magnetic fields. Field tests at a bridge pier revealed how steel components affected the geomagnetic field. While DK reduced calculations, its sensitivity to changing magnetic fields slightly increased measurement errors compared to DU.

Tang et al. (2019) introduced and validated two types of smart rocks for bridge scour monitoring, examining their influence on the geomagnetic field and creating algorithms for precise localization. Field validation in Rolla, MO, USA, revealed how the magnetic field changed with distance from the smart rocks and demonstrated the effectiveness of the localization algorithm. It also highlighted differences between the two smart rock systems in terms of measurement points needed for accurate positioning.

Li et al. (2021) explored the use of multiple smart rocks to predict bridge pier scour depth, proposing algorithms for their precise localization and considering ambient magnetic field effects. Field tests in California, USA, and numerical

simulations revealed how steel rebars influenced the magnetic field dispersion around the bridge pier and showcased the interaction between these rocks, which decayed exponentially with increasing relative distance.

Tang et al. (2023) presented an innovative Semi-active Smart Rock Technology (SSRT) aimed at enhancing scour depth sensing around bridge piers. By utilizing a cylindrical magnet encased in concrete and employing field experiments, the system demonstrated improved accuracy in measuring scour depth through remote-controlled magnet rotation and analysis of magnetic field variations.

2. Methodology

In this study, the scouring characteristics of variously shaped and sized scaled model bridge piers installed in a uniform non-cohesive bedding material within a spacious flume are explored. By conducting a series of experiments and analyzing the obtained data, the study assesses the scour and erosion potential associated with various pier configurations. Several key variables like the effect of shape, size, flow rate, and time of exposure are addressed. The findings from this investigation contribute valuable insights into understanding the complex dynamics of scouring around bridge piers and provide important implications for hydraulic engineering and bridge design practices. This research paper focuses on modeling the scour patterns around bridge piers using SURFER 3D (Bresnahan & Dickenson, 2002) software. The study utilizes a 5-meter Digital Terrain Model (DTM) (Galin et al., 2019) as test data to compare different interpolation results, and subsequently, evaluate their accuracy. Interpolation methods are employed to estimate the heights of specific points of interest by considering the elevation data from neighboring points. The investigation seeks to improve the understanding and evaluation of interpolation techniques for the effective representation of scour patterns in bridge pier hydraulics.

A total of forty experiments were carried out, encompassing a variety of conditions. The tests were conducted over two time durations: 30 min, and 60 min, using two different discharge settings. After each experiment, the bed was meticulously leveled and prepared for the subsequent trial. These experiments were systematically based on four key parameters: the shape of the pier, the size of the pier, the discharge rate in the channel, and the duration of the experiment. The procedural framework is organized in **Figure 3**.

A uniform bed material was sieved and poured into the test section of the flume. The thickness of the bed material was 30 cm, and the slope of the bed was adjusted. The geometric standard deviation (σ_s) is slightly smaller than 1.3, and consequently, sediment distribution may be defined as uniform for this value. Pier spacing, flume dimensions, and sediment characteristics are kept constant throughout the experiments. Local scour evolution in time, approach velocity, and flow depth with sediment size and grading are examined.
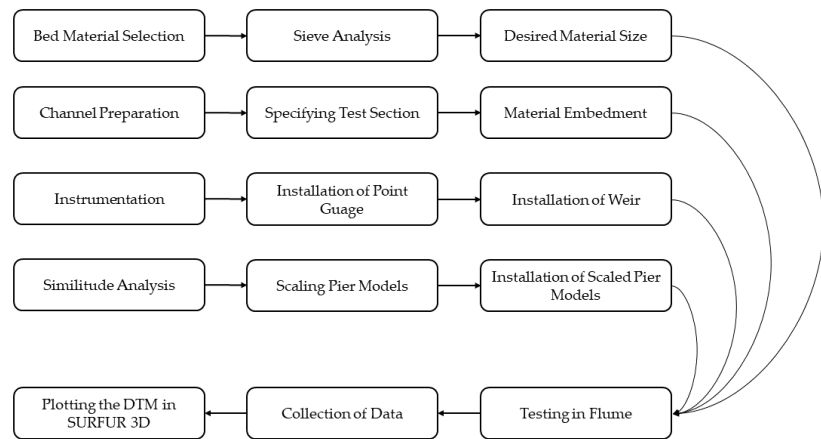
Figure 3. Methodological framework.

2.1. Gradation analysis of the selected material

Two types of material samples were gathered and subjected to sieve analysis as per ASTM D-6913 (American Society for Testing and Materials, 2004) to examine the sediment gradation used in the flume's test section. One out of the two materials was too coarser ($D_{50} = 0.85$) to be used. As sediment size plays a critical role in influencing scour depth and scour hole dimensions. The median size of sediment, represented as D_{50} of 0.52 was used in the experiments. The particle size distribution (PSD) is given in **Figure 4**. The soil was classified as silty sand (SM) according to the unified soil classification system (USCS) (Daryati et al., 2019).

(a)   **(b)**
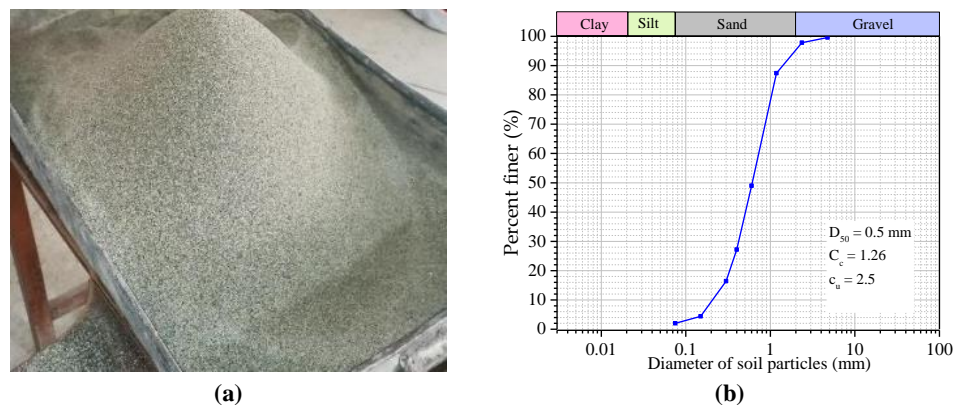
Figure 4. Soil used in this study **(a)** general picture of the soil; **(b)** gradation curve.

2.2. Channel preparation

The hydraulics laboratory at the University of Engineering and Technology, Peshawar, utilizes a flume for conducting experiments. The flume is 15.85 m long, 0.30 m wide, and 0.45 m deep. It includes a centrifugal pump, three water tanks, inflow and outflow control valves, a main flume, a weir, and a sump tank. Water is recirculated from the tanks through the pump into the flume for testing. The flume is equipped with a point gauge to measure scour depth, while a rectangular weir is strategically installed at the test section's end to gauge flow rate and prevent sediment from entering the pump. Essential modifications like the installation of a testing chamber, flow meter, and bed material were made to enhance the flume's performance.

A dedicated test section, 1.37 m in length, was prepared for pier model installation, commencing 4.57 m from the upstream starting point. To ensure smooth water flow and minimize turbulence, glass sheets were placed upstream and downstream of the test section, serving as the datum bed over which water flows and readings are taken. Due to the presence of fine sediment in the test section, the water's movement over the glass bed at the entrance eroded the sand, causing disruption to the local scour depth around the model bridge pier. To mitigate this issue, a small amount of gravel was placed at the bed's start. At the test section's end of the flume, another glass sheet was installed to stabilize the section and prevent sediment transport downstream, which could be eroded due to scouring around the model bridge pier. A point gauge was utilized to measure the scour depth on all sides of the pier. **Figure 5** provides an illustration of the flume and its components.

(a)

(b)

(c)

(d)

(e)

(f)

Figure 5. Flume used in this study and its various sections; **(a)** sketch of the flume; **(b)** general view of the flume; **(c)** meter gauge used for measuring scour depth; **(d)** sheet of glass installed downstream to prevent erosion of sediments; **(e)** flow control valve at upstream of flume; **(f)** flow control valve at downstream of flume.

2.3. Pier model preparation

The scale of the model was selected with respect to the width of the flume (1:30) (Khan et al., 2017). Five different types of models were used for conducting the experiments: (a) Elliptical (76.2 mm × 127 mm) bridge pier model; (b) square bridge pier of size (76.2 mm × 76.2 mm); (c) square bridge pier of size (127 mm × 127 mm); (d) diamond bridge pier of size (76.2 mm × 76.2 mm); (e) diamond bridge pier of size (127 mm × 127 mm). These shapes were selected to better present the pier shapes used commonly by engineers (Vijayasree et al., 2019). The modeled bridge piers are given in **Figure 6**.

| (a) | (b) | (c) |
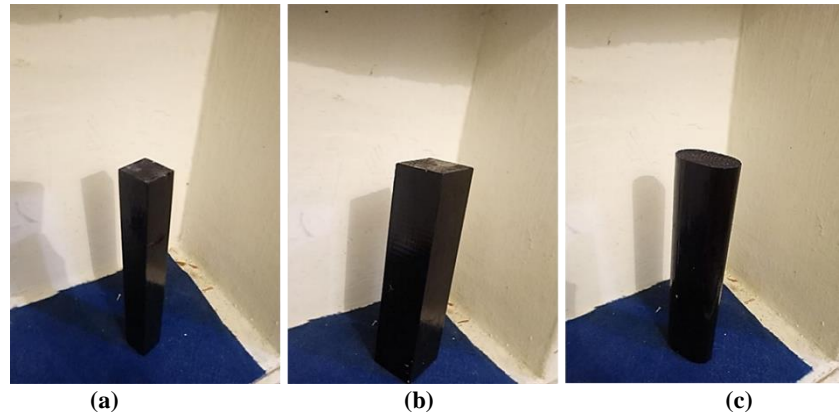
Figure 6. Pier model used in experiments, **(a)** square; **(b)** diamond; **(c)** elliptical.

2.4. Similitude analysis

Laboratory models serve as simplified and scaled-down representations to study specific phenomena under controlled and simplified conditions. However, to ensure the validity of these models and their relevance to real-world structures, it is essential to establish a relationship between them. To achieve this goal, a similitude analysis was carried out, applying Froude number similarity (Banazadeh & Hajipouzadeh, 2019). Froude number similarity is especially relevant for models involving free-surface flow. In the following section, we established relationships for similitude analysis based on Froude's number similarity, where the Froude number (F_r) is represented by Equation (1).

$$Fr = \frac{V}{\sqrt{g \times y}} \tag{1}$$

where, V refers to the velocity of the flow, y is the flow depth, and g is the gravitational acceleration. It was presumed that Froude number of models is equal to Froude number of prototypes. In this study, the Froude number was computed based on the experimental flow conditions and geometry, subsequently juxtaposed against empirical data sourced from Khan et al. (2017). The aim was to replicate authentic hydraulic environments within laboratory settings, ensuring comparability between our experiments and natural occurrences. This method facilitated a comprehensive analysis and correlation of our findings with real-world scenarios. In our study, a length scale ratio of 1:30 was utilized for model preparation, aiming for geometric similarity between the model and prototype, crucial for similitude analysis (Equation (2)). While achieving geometric similarity in sediment transport analysis is

challenging due to sediment scaling limitations, other dimensions except for median-sized sediments can be scaled down in bridge pier scour analysis, preserving angles and flow directions (Zhang et al., 2018).

$$L_r = L_p/L_m \qquad (2)$$

2.5. Experimental procedure

The experiments were performed on the flume located in the hydraulic engineering lab of civil engineering department, University of Engineering and Technology (UET) Peshawar. The flume was cleaned, and the test section was filled with the sediments of median size sediment D_{50} = 0.52 mm. The sediment sand, after putting in the test section, was properly leveled before starting the experiment and this leveling was carried out for each experiment separately. Before the start of the first experiment, the water was allowed to flow over the sand bed in the test section and then was allowed to stay for some time in order to fill the air voids with water in the test section (Khan et al., 2017). The experiment started by saturating sand in the test area and carefully positioning the bridge pier at the center to prevent any impact on the scour depth results. Water flow began, controlled by a valve, while time was recorded. We noted the initial bed levels as references for measuring scour depth using a point gauge. After a while, we measured the scour depths around the pier and the dimensions of the scour hole using the gauge and a scale, respectively. All the experiments are performed based on four parameters which are (a) shape of pier; (b) size of pier; (c) discharge in channel; (d) time duration of the experiment. About twenty experiments under clear water conditions were conducted based on these parameters. The experiments were conducted for 30 min and 60 min on two different discharges of 0.0029 and 0.0026 cumecs. After each experiment, the bed was leveled and prepared for the next experiment. The different views are illustrated in **Figure 7**.

| **(a)** | **(b)** | **(c)** |
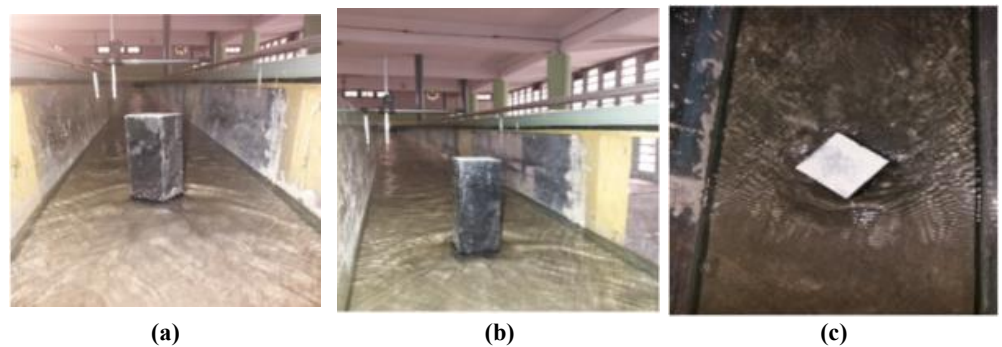
Figure 7. Illustrations of bridge piers in flume **(a)** upstream view; **(b)** downstream view; **(c)** top view.

A series of experiments were conducted in a horizontal flume to investigate flow characteristics over an erodible bed. The flume was 15.85 m long, 0.30 m wide, and 0.45 m deep. To maintain water circulation in the channel, a centrifugal pump with a maximum capacity of 0.2 cumecs was employed. The flow rate within the flume was carefully controlled and preset using a speed control valve connected to the pump system. For discharge measurement, a weir was installed in the supply conduit. The channel's bed was rigid and covered with a layer of uniform sand, approximately 0.20

m thick. The sand particles had a median size of 52 mm and a density of 2650 kg/m^3. The sediment grading exhibited a geometric standard deviation of 1.3. To analyze the flow behavior, velocity profiles were measured when the flume bed was fixed. The results indicated that the flow attained full development after a distance of 5 m from the flume intake.

2.6. Experimental analysis

The results obtained for all experiments have been noted and the readings have been taken on upstream, downstream and both sides of the pier models. Likewise, the dimensions of the scour hole were determined by obtaining horizontal measurements at the upstream, downstream, and sides of the pier model. The test section is graphically represented in **Figure 8**.
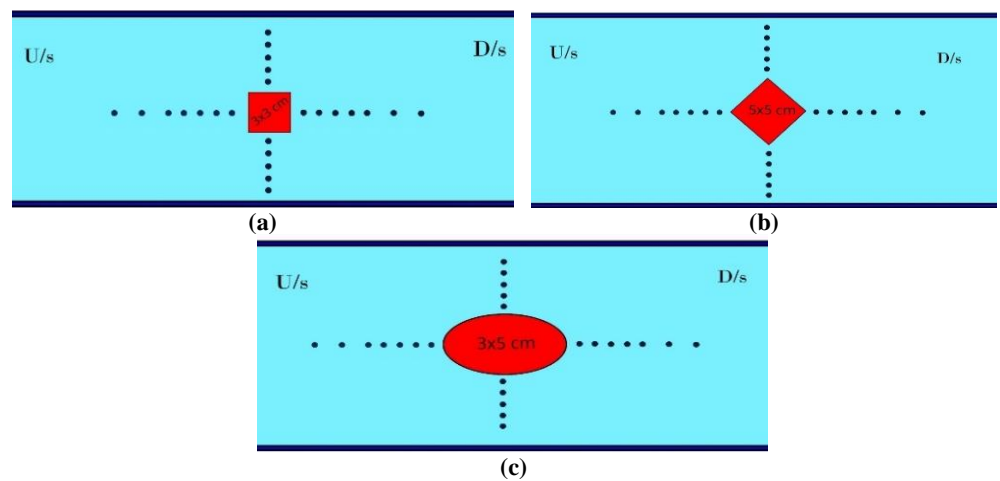
Figure 8. Graphical representation of the flume's test section and the model piers (top view), **(a)** 3 × 3 cm^2 square pier; **(b)** 5 × 5 cm^2 diamond; **(c)** 3 × 5 cm^2 elliptical.

3. Results

Upon concluding each experiment, comprehensive measurements were conducted to determine the scour depth and dimensions of the scour hole, employing both a roller and point gauge. In addition to these primary parameters, supplementary data were gathered with the specific intent of facilitating the creation of contour maps representing the scour hole. In this research, we collected depth measurements at specific spots like the pier face, the edges of the scour hole, and points in between. These readings were paired with their respective distances. The upcoming part of this paper dives into a thorough talk about the contour maps we created based on this data.

3.1. Pier shape versus local scour

It has been observed that upstream (U/S), downstream (D/S), left stream (L/S) and right stream (R/S) scour depth alters with changing the shape of the pier. Three different shapes of piers, i.e., square, diamond and elliptical are experimented and it is evident that scour depth reduces in diamond shaped pier when compared with square shaped pier while keeping other parameter like time (*t*), discharge (*Q*), and size constant.

In comparison of diamond and elliptical shapes, scour depth further reduces in case of elliptical pier when other parameters are kept constant. The upstream scour depth observed in square pier is 48 mm, 40.5 mm in case of diamond while 34 mm has been measured in elliptical pier. The results are summarized in **Figure 9** respectively.
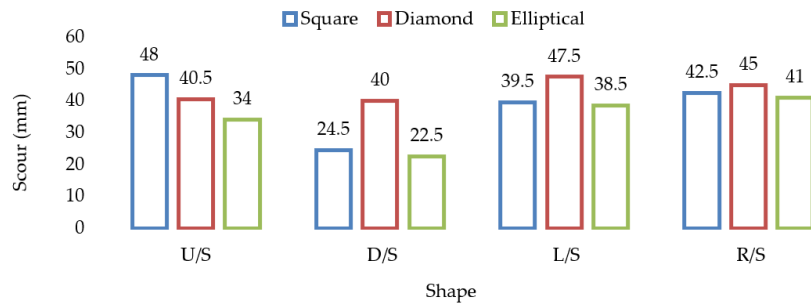
Figure 9. Comparison of local scour for square, diamond and elliptical shapes of the bridge pier models.

These findings highlight the importance of pier shape in influencing local scour characteristics, suggesting that streamlined pier shapes may mitigate scour-related concerns. Jalal and Hassan (2020) using Flow-3D simulation obtained similar results and showed that rectangular piers had the maximum depth of scour, with the maximum scour depth occurring at a pier width ratio of 0.2.

Pier shape is a significant factor influencing local scour depth. This information can be used by researchers and engineers to design bridge piers and other hydraulic structures that are more resistant to scour.

3.2. Pier size versus local scour

Pier size is another major parameter which affects the scour depth. It has been concluded from the experiments that scour depth and scour hole increases by increasing the size of the pier by keeping other parameters constant (time, flow rate, and shape). The square pier, measuring 3×3 cm^2, shows a scour depth of 48 mm on the upstream side. In contrast, the square pier of dimensions 5×5 cm^2 exhibits a scour depth of 60.5 mm on its upstream face, as illustrated in **Figure 10**.
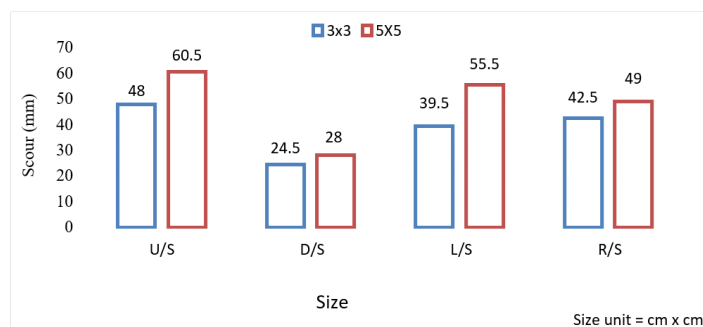
Figure 10. Comparison of local scour different sizes of the square bridge pier models.

These results highlight the significant impact of pier size on local scour depth.

The scour depth and scour hole area increase with increasing pier size, even when other parameters such as time, flow rate, and pier shape are kept constant. This is because larger piers have a larger projected area and therefore create a greater obstruction to the flow of water. This increased obstruction leads to higher velocities and turbulence around the pier, which in turn erodes the bed sediment and creates a deeper scour hole.

Findings from the study of Aly and Dougherty (2021) suggest that engineers can reduce the risk of local scour around bridge piers by using smaller piers and by implementing scour countermeasures such as delta vanes or angled plate footings. The connection between pier size and scour depth is intricate and relies on various factors: flow conditions, bed sediment traits, and pier shape. Still, a broad pattern emerges— larger piers tend to cause more scouring. This study's insights offer engineers a basis for creating design guidelines to reduce scour risk in hydraulic structures. For instance, they might opt for smaller piers or apply protective measures like riprap or scour holes.

3.3. Time of exposure versus local scour

As scour is a temporal process, the scour depth increases by increasing the time of flow around the bridge pier until equilibrium scour depth is achieved. The experimental results of scour depth w.r.t time by keeping other parameters constant has been observed and presented in **Figure 11** for square pier of size 3×3 cm^2.
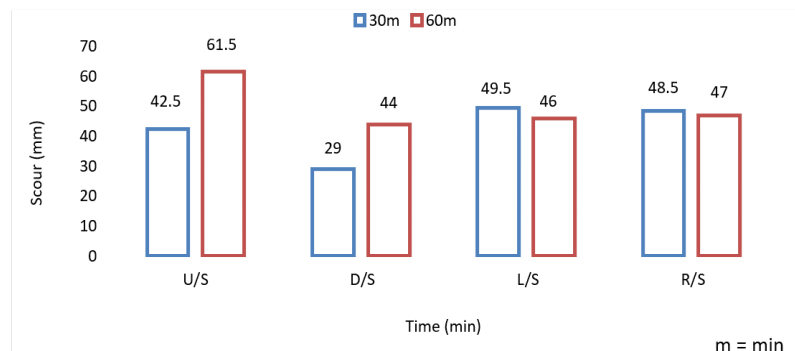
Figure 11. Comparison of local scour for different time periods for square pier of size 3×3 cm^2.

This study highlights how the time something is exposed is a big deal when it comes to how deep the local scour gets. The longer something's exposed, the deeper the scour tends to get. Also, when the flow's faster and the bed sediment isn't cohesive, things hit an equilibrium scour depth faster. Plus, those scour holes can end up trapping stuff like sediment and debris, making the scour even deeper over time. Engineers planning bridges and hydraulic structures need to pay close attention to how long things are exposed, especially in places where scouring is a worry.

The local scour process, as categorized by Ettema (1980), involves three phases: initial, principal, and equilibrium, with the equilibrium phase representing a point where scour development stabilizes. The concept of equilibrium in scour remains debated, with some suggesting it may take an infinite amount of time, while others offer varied criteria for defining it. This underscores the complex relationship between time of exposure and achieving equilibrium, highlighting the necessity for precise

criteria in its definition (Coleman, 2005; Grimaldi et al., 2009).

3.4. Channel flow rate versus local scour

As the discharge in the channel increases, there's a simultaneous elevation in the scour depth around the bridge pier. The results for square pier of size 3×3 cm^2 are presented in **Figure 12** where the maximum local scour occurs at the upstream (U/S) having depth of 61.5 mm for a discharge of 0.0029 cumecs and 48 mm for a discharge of 0.0026 cumecs. The experimental results are summarized in **Table 1**.
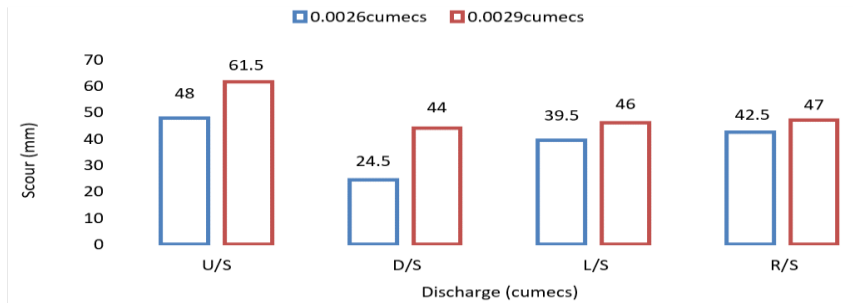
Figure 12. Comparison of local scour around square bridge piers for different flow rates.

Table 1. Summary of the experiments in terms of U/S, D/S, L/S and R/S local scour.

S. No.	Time (min)	Size cm²	Shape	Discharge (cumecs)	Local scour (mm)			
					U/S	D/S	L/S	R/S
1	60	3 × 3	Square	0.0026	34.5	12.5	25.5	21.5
2	60	5 × 5	Square	0.0026	61	29.5	48.5	54.5
3	60	3 × 3	Diamond	0.0026	34.5	42.5	52.5	43.5
4	60	5 × 5	Diamond	0.0026	52.5	49.5	64.5	68
5	60	3 × 5	Elliptical	0.0026	34.5	19.5	41	35.5
6	60	3 × 3	Square	0.0029	42.5	29	49.5	48.5
7	60	5 × 5	Square	0.0029	77	37	67	74
8	60	3 × 3	Diamond	0.0029	29.5	30	44.5	39
9	60	5 × 5	Diamond	0.0029	64	50	77.5	73
10	60	3 × 5	Elliptical	0.0029	34	17	45.5	40.5
11	30	3 × 3	Square	0.0026	48	24.5	39.5	42.5
12	30	5 × 5	Square	0.0026	60.5	19	55.5	49
13	30	3 × 3	Diamond	0.0026	40.5	40	47.5	45
14	30	5 × 5	Diamond	0.0026	54.5	43.5	57.5	66
15	30	3 × 5	Elliptical	0.0026	34	22.5	38.5	41
16	30	3 × 3	Square	0.0029	61.5	44	46	47
17	30	5 × 5	Square	0.0029	73.5	30.5	61.5	61.5
18	30	3 × 3	Diamond	0.0029	27.5	26	40.5	41.5
19	30	5 × 5	Diamond	0.0029	58.5	57.5	73.5	68
20	30	3 × 5	Elliptical	0.0029	12.5	32	36	33.5

The findings underscore how crucial the channel's flow rate is for local scouring. When the flow rate goes up, so does the local scour depth, especially in the clear-water scour regime. This happens because higher flow rates mean faster and more turbulent water around the pier, leading to more erosion of the bed sediment. However, this link between flow rate and scour depth is intricate and hinges on various factors like the bed sediment, pier shape, and how long things are exposed.

However, the general trend is that local scour depth increases with increasing flow rate. Several studies, including Melville & Coleman (2000); Raudkivi and Ettema (1983); and Raudkivi (1986) underline a significant linear relationship between equilibrium scour depth and clear water regime flow velocity. Melville's extensive data set confirms this pattern, also revealing a similar linear increase in the timescale of scour, peaking at critical velocity, which underscores the link between flow rate, regime transitions, and the evolution of local scour.

3.5. Local scour contour profiles using SURFER

The research findings, as depicted by the contour maps presented in **Figure 13**, reveal distinctive trends in the scour hole dimensions for different shaped piers. Specifically, when comparing an elliptical shaped pier to a square pier of equal size, the former exhibits a smaller scour hole. Conversely, in the case of a diamond shaped pier, the scour hole is larger than that of a square pier of the same dimensions.

The study highlights that a square pier with dimensions of $3 \times 3 \text{cm}^2$ experiences a smaller scour hole compared to a square pier with dimensions of $5 \times 5 \text{cm}^2$, both under the same discharge conditions. Similarly, for a discharge of 0.0026 cumecs, the scour hole in a square pier is smaller than when subjected to a discharge of 0.0029 cumecs, while maintaining the same pier size.

This research offers crucial insights into how pier shape, size, and discharge all work together to create scour holes. Understanding these interactions is vital for improving the design and stability of hydraulic structures in different engineering uses.
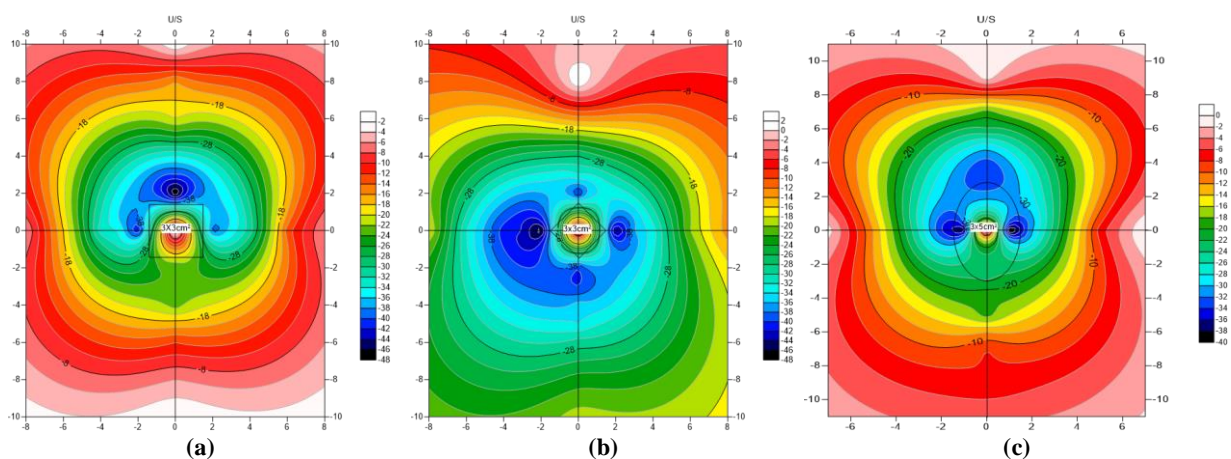
Figure 13. (*Continued*).
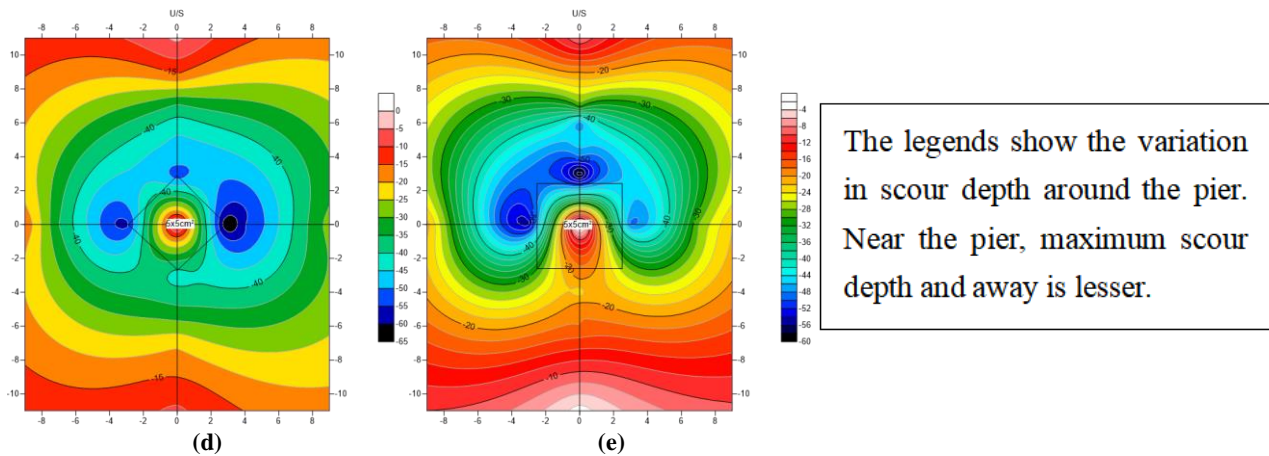
Figure 13. Illustrations of scour's contours around different shaped model bridge piers **(a)** 3×3 cm^2 square shaped bridge pier; **(b)** 3×3 cm^2 diamond shaped bridge pier; **(c)** 3×5 cm^2 elliptical shaped bridge pier; **(d)** diamond pier having size 5×5 cm^2; **(e)** square pier having size 5×5 cm^2.

4. Discussion

The research focuses on scour depth changes at bridge piers through lab experiments with varying flow rates. It evaluated five pier designs under clear water conditions, measuring scour development and final depth. A predictive method for real-world scenarios showed efficiency and accuracy in controlled experiments.

This research uses experiments to mimic real field conditions accurately. Physical models resembling actual bridge piers and riverbeds were crafted in a flume, replicating bed configurations and water conditions. These models effectively imitated scouring patterns observed in real scenarios, proving their usefulness in hydraulic engineering research. The study pinpointed key factors affecting scouring—flow velocity, sediment concentration, and pier shape—essential for designing anti-scour measures around bridge piers. This approach yields data closely resembling real scenarios, boosting the findings' reliability and practicality.

Moreover, the control over various parameters, like flow velocity, sediment traits, and pier shapes, grants a significant advantage. This control allows systematic studies, isolating individual factors to measure their impact on scour. Such precision enhances our understanding of the processes behind scour development.

Through experimental investigations, visual observation of the scour evolution around different shaped bridge piers. High-resolution imaging techniques such as DTM using SURFER captured the scouring pattern around the different sides of piers, offering valuable insights into the temporal and spatial dynamics of scour development. Visual representations aid in comprehending scour patterns and identifying critical flow conditions leading to maximum scour depths. While the experimental investigation provided valuable insights into local scours around different shaped bridge piers, certain methodological limitations should be acknowledged. Scale effects inherent in the laboratory setup, simplified steady clear-water conditions, and the absence of complex bridge configurations may affect the generalizability of findings. The study's emphasis on short-term scour dynamics within specific parameter ranges might limit its relevance to varied hydraulic conditions. The potential influence of hydrodynamic interactions and the sensitivity to test duration emphasizes the

importance of careful interpretation. Future research could overcome these limitations by including more diverse flow patterns, intricate bridge layouts, and a wider range of influencing factors. This expansion could strengthen the study's reliability and practicality in real-world scenarios. The model predictions derived from this experimental investigation offer valuable insights with potential implications for future applications in hydraulic engineering and bridge design. Variations in local scour depths across different pier shapes offer insights for optimizing bridge designs and mitigating scour risks. These findings aid engineers in selecting more resilient pier shapes, enhancing bridge stability. The study's focus on critical parameters like flow rate, exposure time, and pier size opens avenues for refining predictive models. This knowledge can shape design guidelines, improve risk assessment practices, and contribute to resilient infrastructure development near waterways. As further research explores scour complexities, these insights will aid in designing safer, durable bridges for dynamic hydraulic conditions.

Key parameters to reduce local scour

Understanding how local scour affects bridge piers is crucial for stronger structures. This research pinpoints how pier shape impacts scour depth, paving the way for smarter designs that resist floods. Fine-tuning pier shapes can fortify bridges against strong vortices of water. The key factors such as pier shape, flow rate and pier size, time of exposure studied here, shape how scour works. Using these insights in designs could protect piers better, making this study a key resource for creating safeguards against scour's impact on bridges.

5. Conclusions

This study has been conducted to investigate the impact of different shape piers models of different size on the scouring depth using laboratory hydraulic flume experiments under steady clear-water conditions. The analysis considered various flow rates and discharge levels to identify the most efficient shape with reduced local scour. The following conclusion has been drawn from the experimental results.

- The elliptical shape stands out as the most effective design in mitigating bridge pier scours in comparison with square and diamond shape piers. The local scour depths around elliptical piers were 29.16% less, and around diamond piers, approximately 16.05% less than the scour depth observed around square piers of identical dimensions.

- For both square and elliptical shapes, maximum scour occurs upstream of the pier. In contrast, the diamond-shaped pier experiences its peak scouring on the sides due to increased turbulence generation at these locations.

- The diamond shape proves to be more advantageous than the square, as it demonstrates reduced scouring upstream of the pier. This finding underscores the significance of innovative pier geometry in minimizing potential risks.

- The test findings also unveiled the significant influence of pier size on scouring. Enlarging the pier dimensions from 3×3 cm^2 to 5×5 cm^2 led to an increase in scour depth by 26.04 %.

- Scour phenomena exhibit a direct and proportional relationship with discharge

rates. Higher discharge leads to intensified scouring, emphasizing the role of water flow in shaping scour patterns i.e., raising the discharge from 0.0026 cumecs to 0.0029 cumecs resulted in a notable 28.13% increase in scouring depth for piers of the same size.

- To ensure optimal bridge performance throughout its lifespan, predetermining the depth of the scour hole surrounding the bridge pier is imperative. This proactive approach safeguards against unforeseen scour developments that could compromise the load-bearing capacity of foundation piles in the future.

- These scientific conclusions illuminate the intricate dynamics of bridge pier scour and offer valuable insights for the design and maintenance of resilient infrastructure. By harnessing the knowledge gleaned from this research, engineers can better navigate the challenges posed by hydraulic forces, leading to safer and more enduring bridges that withstand the test of time and nature.

Conflict of interest: The authors declare no conflict of interest.

References

Aly, A. M., & Dougherty, E. (2021). Bridge pier geometry effects on local scour potential: A comparative study. Ocean Engineering, 234, 109326. https://doi.org/10.1016/j.oceaneng.2021.109326

American Society for Testing and Materials. (2004). Committee D18 on Soil and Rock, Standard test methods for particle-size distribution (gradation) of soils using sieve analysis. ASTM International.

Brunner, G. W. (2016). HEC-RAS River Analysis System: Hydraulic Reference Manual, Version 5.0. US Army Corps of Engineers–Hydrologic Engineering Center, vol. 547.

Banazadeh, A., & Hajipouzadeh, P. (2019). Using approximate similitude to design dynamic similar models. Aerospace Science and Technology, 94, 105375. https://doi.org/10.1016/j.ast.2019.105375

Beg, M. (2010). Characteristics of Developing Scour Holes around Two Piers Placed in Transverse Arrangement. Scour and Erosion. https://doi.org/10.1061/41147(392)6

Bresnahan, T., Dickenson, K. (2002). Surfer 8 self-paced training guide. Golden Software Inc.

Bakht, B., & Jaeger, L. G. (1992). Simplified methods of bridge analysis for the third edition of OHBDC. Canadian Journal of Civil Engineering, 19(4), 551–559. https://doi.org/10.1139/l92-066

Chen, Y., Tang, F., Li, Z., Chen, G., & Tang, Y. (2018). Bridge scour monitoring using smart rocks based on magnetic field interference. Smart Materials and Structures, 27(8), 085012. https://doi.org/10.1088/1361-665x/aacbf9

Coleman, S. E. (2005). Clearwater Local Scour at Complex Piers. Journal of Hydraulic Engineering, 131(4), 330–334. https://doi.org/10.1061/(asce)0733-9429(2005)131:4(330)

Daryati, D., Widiasanti, I., Septiandini, E., Ramadhan, M. A., Sambowo, K. A., & Purnomo, A. (2019). Soil characteristics analysis based on the unified soil classification system. Journal of Physics: Conference Series, 1402(2), 022028. https://doi.org/10.1088/1742-6596/1402/2/022028

Dahe, P., Kharode, S. (2015). Evaluation of scour depth around bridge piers with various geometrical shapes. Evaluation, 2(7): 41–48.

Deng, L., & Cai, C. S. (2010). Bridge Scour: Prediction, Modeling, Monitoring, and Countermeasures—Review. Practice Periodical on Structural Design and Construction, 15(2), 125–134. https://doi.org/10.1061/(asce)sc.1943-5576.0000041

Dey, S. (1997a). Local scour at piers, part I: a review of developments of research. Int. J. Sediment Res., Beijing, China, 12(2), pp. 23–46.

Dey, S. (1997b). Local scour at piers, part II: bibliography. Int. J. Sediment Res, 12(2): 47–57.

Dargahi, B. (1982). Local scouring around bridge piers—A review of practice and theory. Bull, vol. 114.

Eddine, M. S., & Arjomandi, K. (2020). Assessment of the Accuracy of Bridge Evaluation Methods Outlined by CHBDC. presented at the Transportation Association of Canada 2020 Conference and Exhibition-The Journey to Safer Roads.

Ettema, R. (1980). Scour at bridge piers. 1980.

Farooq, R., Ghumman, A. R., & Hashmi, H. N. (2017). Influence of pier modification techniques for reducing scour around bridge piers. International Journal of Civil and Environmental Engineering, 11(4), 462–468.

Grimaldi, C., Gaudio, R., Calomino, F., & Cardoso, A. H. (2009). Countermeasures against Local Scouring at Bridge Piers: Slot and Combined System of Slot and Bed Sill. Journal of Hydraulic Engineering, 135(5), 425–431. https://doi.org/10.1061/(asce)hy.1943-7900.0000035

Galin, E., Guérin, E., Peytavie, A., Cordonnier, G., Cani, M., Benes, B., & Gain, J. (2019). A Review of Digital Terrain Modeling. Computer Graphics Forum, 38(2), 553–577. Portico. https://doi.org/10.1111/cgf.13657

Gampathi, G. A. P. (2010). Suitable Bridge Pier Section for a Bridge over a Natural River. Engineer: Journal of the Institution of Engineers, Sri Lanka, 43(3), 44. https://doi.org/10.4038/engineer.v43i3.6973

Heller, V. (2011). Scale effects in physical hydraulic engineering models. Journal of Hydraulic Research, 49(3), 293–306. https://doi.org/10.1080/00221686.2011.578914

Ismael, A., Gunal, M., & Hussein, H. (2015). Effect of Bridge Pier Position on Scour Reduction According to Flow Direction. Arabian Journal for Science and Engineering, 40(6), 1579–1590. https://doi.org/10.1007/s13369-015-1625-x

Ismail, S. (2009). Evaluation of local scour around bridge piers (River Nile Bridges as Case Study). Thirteenth International Water Technology Conference, IWTC, Citeseer, pp. 1249–1260.

Jalal, H. K., & Hassan, W. H. (2020). Effect of Bridge Pier Shape on Depth of Scour. IOP Conference Series: Materials Science and Engineering, 671(1), 012001. https://doi.org/10.1088/1757-899x/671/1/012001

Khan, M., Tufail, M., Ajmal, M., Haq, Z. U., & Kim, T.-W. (2017). Experimental Analysis of the Scour Pattern Modeling of Scour Depth Around Bridge Piers. Arabian Journal for Science and Engineering, 42(9), 4111–4130. https://doi.org/10.1007/s13369-017-2599-7

Kuchma, D. A., Hawkins, N. M., Kim, S.-H., Sun, S., & Kim, K. S. (2008). Simplified shear provisions of the AASHTO LRFD Bridge Design Specifications. PCI Journal, 53(3), 53–73. https://doi.org/10.15554/pcij.05012008.53.73

Li, Z., Tang, F., Chen, Y., Hu, X., Chen, G., & Tang, Y. (2021). Field experiment and numerical verification of the local scour depth of bridge pier with two smart rocks. Engineering Structures, 249, 113345. https://doi.org/10.1016/j.engstruct.2021.113345

Lai, J. S., Chang, W. Y., & Yen, C. L. (2009). Maximum Local Scour Depth at Bridge Piers under Unsteady Flow. Journal of Hydraulic Engineering, 135(7), 609–614. https://doi.org/10.1061/(asce)hy.1943-7900.0000044

Lyn, D. A. (2008). Pressure-Flow Scour: A Reexamination of the HEC-18 Equation. Journal of Hydraulic Engineering, 134(7), 1015–1020. https://doi.org/10.1061/(asce)0733-9429(2008)134:7(1015)

Lagasse, P. F., Schall, J. D., Johnson F., et al. (1995). Stream stability at highway structures. United States. Federal Highway Administration. Office of Technology Applications.

Melville, B., Coleman, S. (2000). Bridge scour Water Resources Publications. LLC, Colorado, USA; 2000.

Masjedi, A., Shafaei BEJESTAN, M., & Esfandi, A. (2010). Experimental study on local scour around single oblong pier fitted with a collar in a 180 degree flume bend. International Journal of Sediment Research, 25(3), 304–312. https://doi.org/10.1016/s1001-6279(10)60047-9

Panici, D., & de Almeida, G. A. M. (2018). Formation, Growth, and Failure of Debris Jams at Bridge Piers. Water Resources Research, 54(9), 6226–6241. Portico. https://doi.org/10.1029/2017wr022177

Richardson, E. V., Davis, S. R. (1995). Evaluating scour at bridges. United States. Federal Highway Administration. Office of Technology Applications.

Raudkivi, A. J. (1986). Functional Trends of Scour at Bridge Piers. Journal of Hydraulic Engineering, 112(1), 1–13. https://doi.org/10.1061/(asce)0733-9429(1986)112:1(1)

Raudkivi, A. J., & Ettema, R. (1983). Clear-Water Scour at Cylindrical Piers. Journal of Hydraulic Engineering, 109(3), 338–350. https://doi.org/10.1061/(asce)0733-9429(1983)109:3(338)

Shahriar, A. R., Ortiz, A. C., Montoya, B. M., & Gabr, M. A. (2021). Bridge Pier Scour: An overview of factors affecting the phenomenon and comparative evaluation of selected models. Transportation Geotechnics, 28, 100549. https://doi.org/10.1016/j.trgeo.2021.100549

Sotiropoulos, F., Diplas, P., Khosronejad, A. (2012). Scour around Hydraulic Structures. In Handbook of Environmental Fluid Dynamics, Volume Two, CRC Press, 2012, pp. 88–103.

Tang, Y., Chen, Y., Tang, F., Liang, Y., & Li, Z. (2023). Field experiment of a novel semi-active smart rock system for sensing bridge scour depth. Structures, 53, 1150–1159. https://doi.org/10.1016/j.istruc.2023.05.021

Tang, F., Chen, Y., Li, Z., Hu, X., Chen, G., & Tang, Y. (2019). Characterization and field validation of smart rocks for bridge scour monitoring. Structural Health Monitoring, 18(5–6), 1669–1685. https://doi.org/10.1177/1475921718824944

Tejada, S. (2014). Effects of blockage and relative coarseness on clear water bridge pier scour.

Vijayasree, B. A., Eldho, T. I., Mazumder, B. S., & Ahmad, N. (2019). Influence of bridge pier shape on flow field and scour geometry. International Journal of River Basin Management, 17(1), 109-129.

Zhang, G., Liu, Y., Liu, J., Lan, S., & Yang, J. (2022). Causes and statistical characteristics of bridge failures: A review. Journal of Traffic and Transportation Engineering (English Edition), 9(3), 388–406. https://doi.org/10.1016/j.jtte.2021.12.003

Zhang, L., Wang, P., Yang, W., Zuo, W., Gu, X., & Yang, X. (2018). Geometric Characteristics of Spur Dike Scour under Clear-Water Scour Conditions. Water, 10(6), 680. https://doi.org/10.3390/w10060680

Zevenbergen, L. W. (2010). Comparison of the HEC-18, Melville, and Sheppard Pier Scour Equations. Scour and Erosion. https://doi.org/10.1061/41147(392)108